NASA/TP-1998-207645

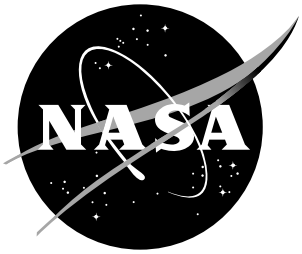

Evaluation of Composite Honeycomb Sandwich Panels Under Compressive Loads at Elevated Temperatures

Sandra Walker
Langley Research Center, Hampton, Virginia

April 1998

The NASA STI Program Office ... in Profile

Since its founding, NASA has been dedicated to the advancement of aeronautics and space science. The NASA Scientific and Technical Information (STI) Program Office plays a key part in helping NASA maintain this important role.

The NASA STI Program Office is operated by Langley Research Center, the lead center for NASA's scientific and technical information. The NASA STI Program Office provides access to the NASA STI Database, the largest collection of aeronautical and space science STI in the world. The Program Office is also NASA's institutional mechanism for disseminating the results of its research and development activities. These results are published by NASA in the NASA STI Report Series, which includes the following report types:

- TECHNICAL PUBLICATION. Reports of completed research or a major significant phase of research that present the results of NASA programs and include extensive data or theoretical analysis. Includes compilations of significant scientific and technical data and information deemed to be of continuing reference value. NASA counter-part of peer reviewed formal professional papers, but having less stringent limitations on manuscript length and extent of graphic presentations.

- TECHNICAL MEMORANDUM. Scientific and technical findings that are preliminary or of specialized interest, e.g., quick release reports, working papers, and bibliographies that contain minimal annotation. Does not contain extensive analysis.

- CONTRACTOR REPORT. Scientific and technical findings by NASA-sponsored contractors and grantees.

- CONFERENCE PUBLICATION. Collected papers from scientific and technical conferences, symposia, seminars, or other meetings sponsored or co-sponsored by NASA.

- SPECIAL PUBLICATION. Scientific, technical, or historical information from NASA programs, projects, and missions, often concerned with subjects having substantial public interest.

- TECHNICAL TRANSLATION. English-language translations of foreign scientific and technical material pertinent to NASA's mission.

Specialized services that help round out the STI Program Office's diverse offerings include creating custom thesauri, building customized databases, organizing and publishing research results ... even providing videos.

For more information about the NASA STI Program Office, see the following:

- Access the NASA STI Program Home Page at ***http://www.sti.nasa.gov***

- E-mail your question via the Internet to help@sti.nasa.gov

- Fax your question to the NASA Access Help Desk at (301) 621-0134

- Phone the NASA Access Help Desk at (301) 621-0390

- Write to:
  NASA Access Help Desk
  NASA Center for AeroSpace Information
  7121 Standard Drive
  Hanover, MD 21076-1320

NASA/TP-1998-207645

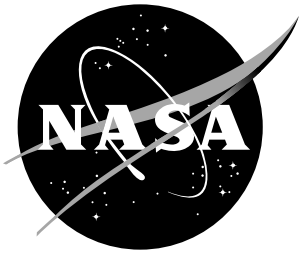

Evaluation of Composite Honeycomb Sandwich Panels Under Compressive Loads at Elevated Temperatures

Sandra Walker
Langley Research Center, Hampton, Virginia

National Aeronautics and
Space Administration

Langley Research Center
Hampton, Virginia 23681-2199

April 1998

Available from the following:

NASA Center for AeroSpace Information (CASI)
7121 Standard Drive
Hanover, MD 21076-1320
(301) 621-0390

National Technical Information Service (NTIS)
5285 Port Royal Road
Springfield, VA 22161-2171
(703) 487-4650

Abstract

Fourteen composite honeycomb sandwich panels were tested to failure under compressive loading. The test specimens included panels with both eight and twenty-four ply graphite-bismaleimide composite facesheets and both titanium and graphite-polyimide core materials. The panels were designed to have the load introduced through fasteners attached to pairs of steel angles on the ends of the panels to simulate double shear splice joints. The unloaded edges were unconstrained. Test temperatures included room temperature, 250°F, and 300°F. For the room and 250°F temperature tests, the 24-ply specimen failure strains were close to the unnotched allowable strain values and failure loads were well above the design loads. However, failure strains much lower than the unnotched allowable strain values, and failure loads below the design loads were observed with several of the 8-ply specimens. For each individual test temperature, large variations in the failure strains and loads were observed for the 8-ply specimens. Dramatic decreases in the failure strains and loads were observed for the 24-ply specimens as the test temperature was increased from 250°F to 300°F. Due to initial geometric imperfections, all specimens exhibited varying degrees of bending prior to failure. All 8-ply specimens appeared to have failed in a facesheet strength failure mode for all test temperatures. The 24-ply specimens displayed appreciably greater amounts of bending prior to failure than the 8-ply specimens, and panel buckling occurred prior to facesheet strength failure for the 24-ply room and 250°F temperature tests. For the two 24-ply specimens tested at 300°F, one panel failed due to facesheet strength and the other due to a disbond between the facesheet and core materials.

Introduction

The development of advanced lightweight structural components is an important requirement for an economically feasible high speed civil transport. Figure 1 displays a conceptual drawing of a high speed civil transport. At supersonic speeds, both the wing and fuselage structure will be exposed to elevated temperature. For an aircraft designed to cruise at Mach 2.4, structural surface temperatures up to 350°F have been predicted (ref. 1). Since material strength and stiffness properties generally degrade at elevated temperatures, the high temperature operating environment challenges structural components to maintain effective load carrying capabilities. The quest for lightweight structural components able to carry high mechanical loads at elevated temperatures has led to the consideration of composite honeycomb sandwich panels for such applications. However, the effect of temperature on the load carrying capability of composite honeycomb sandwich structure is not well understood. Although thermal effects on the individual sandwich components, the composite facesheets, adhesive, and honeycomb cores, have been investigated, interactions between these components in a sandwich panel may exhibit a significantly different temperature dependence.

In the present study, fourteen composite honeycomb sandwich panels were tested at

either; room temperature, 250°F, or 300°F. Each panel was tested to failure under compressive loads at a uniform temperature. The panels were fabricated by Marion Composites under contract with The Boeing Commercial Airplane Group. The panels were tested in the Thermal Structures Laboratory at NASA Langley Research Center.

The purpose of the tests was to evaluate the effect of temperature on the failure mode and load carrying capability of the composite honeycomb panels under investigation. This paper presents test and analysis results from fourteen panels that were tested in compression to 1) evaluate the ability of the composite honeycomb sandwich panels to carry compressive mechanical loads at room and elevated temperatures, 2) determine the effect of temperature on the compressive failure mode of these panels, and 3) evaluate the ability of analysis methods to predict the compressive failure mode and load of the composite honeycomb sandwich specimens.

Test Program

A test program was established to observe the effect of temperature on the failure mode and failure load of structural panels being considered for a high speed civil transport. The focus of this test program was on compression dominated areas of the aircraft where structural response tends to be more complex. Composite honeycomb sandwich panels are being considered for compression wing panels due their structural efficiency. However, there are concerns about the ability of these panels to maintain their structural integrity at elevated temperatures. Interactions between the laminated facesheets, adhesive bonds, and honeycomb core add to the complexity of the problem in predicting failure loads and temperature effects. The fabrication procedure, a co-curing process in the present study, may effect the structural integrity of the panels. In addition, geometric imperfections of the panel, possible non-visible impact damage and fabrication defects (i.e., local areas of disbond between the facesheets and core) exasperate the issue. Although an extensive test program is needed to understand the behavior of a composite honeycomb sandwich panel at elevated temperatures, the present study was limited to fourteen panels.

To introduce the compressive load into the panels, the test specimens were configured with bolted joint connections to simulate double shear splice joints. Each end of the composite honeycomb sandwich panel was potted and attached to a pair of steel angles by two rows of fasteners. The bolted joints provided load paths for the tests which are similar to those expected in joints in a high speed civil transport, but also added more complexity to the tests and increased the difficulty in creating an accurate analytical model.

Panel Design

It is standard practice to design lightweight aircraft sandwich structure for simultaneous failure modes to increase panel structural efficiency. For these particular sandwich panels designed by Boeing, panel buckling and facesheet strength failure were the two possible failure modes having nearly zero margins of safety. Facewrinkling, shear crimping, bolt bending, and bolt shear were ruled out as possible failure modes due to high margins of safety. Pad-up plies were added in the joint area to increase the bearing capability and reduce the risk of bearing failures. The honeycomb core was potted in the joint areas to prevent core crushing from bolt clamp-up. The preliminary design analyses for the panels were conducted with the panels at room temperature. The objective of the testing program is to define the structural performance degradation due to temperature.

Materials selected for the design of the panels were among those being considered for use in a high speed civil transport. The composite facesheet material is an toughened graphite-bismaleimide designated IM7/5260 and manufactured by Cytec Engineering. Two

wing panel concepts were chosen for this study. One concept had minimum thickness 8-ply facesheets representative of a lightly loaded structure and the other concept had 24-ply facesheets representative of a moderately loaded structure. Both the 8-ply and 24-ply laminated facesheets had quasi-isotropic layups.

Cytec BMI X2550G dry film adhesive, with a thickness of 0.01 inches, was used to bond the facesheets to the core. Two core materials with the same cell density and configuration, were selected for direct comparison and evaluation. The core materials were a titanium honeycomb foil of the alloy Ti-3Al-2.5V and a non-metallic honeycomb fabricated by Hexcel Corporation, designated HFT-G-327, which is a bias weave graphite fabric reinforced polyimide honeycomb. Both core materials have a cell size of 3/16 inches and a nominal density of approximately 6 lbs/ft^3.

Test Specimen Descriptions

Fourteen test panels were fabricated by Marion Composites using a proprietary co-curing process developed jointly with Boeing and Marion. A schematic diagram of a panel specimen is shown in Figure 2. The panel length, l, and width, w, are depicted in the front view, and the facesheet thickness, t, and the core depth, c, are depicted in the side view shown in Figure 2. A testing matrix describing all test specimens is provided in Table 1. All panels measured approximately 12 inches wide by 35 inches long with a one inch thick honeycomb core. Four of the panels had 8-ply facesheets with titanium core, four had 8-ply facesheets with graphite-polyimide core, and the remaining six panels had 24-ply facesheets with graphite-polyimide core. All 8-ply specimens had 2.75 inches of the core potted at each end and had steel angles attached with two rows of fasteners using nine 3/16 inch diameter steel bolts per row. Four of the 24-ply specimens had 3.25 inches of the core potted and two rows of fasteners using eight 3/8 inch diameter steel bolts per row, and the remaining two had 3.25 inches of the core potted on the ends but without the bolted joint connections used to simulate a double shear splice joint. In the joint area of the panels, four additional plies were added to the outside of each 8-ply facesheet and eight additional plies were added to the outside of each 24-ply facesheet.

Each specimen was instrumented with strain gauges mounted back-to-back on the outer surfaces of the panel facesheets. The panels tested at elevated temperatures were also instrumented with thermocouples. A typical instrumentation layout used for several of the specimens is shown in Figure 3. The figure displays half of the panel length, where all instrumentation is symmetric about the panel centerline.

Test Apparatus and Procedure

A 500-kip hydraulically-actuated universal test machine was used to load all the test specimens to failure in compression. A photo of one of the failed specimens located in the test machine is shown in Figure 4. Heated platens were mounted through ceramic insulators to the steel compression platens. Loads were applied to the panel through the heated platens and the steel angles on the test specimens as shown in Figure 4. The two unloaded edges were unconstrained. Test data was recorded using a NEFF 470 data acquisition system coupled with a computer to store test data and display real-time data plots.

Prior to heating the panels, ten percent of the predicted compressive strength failure load was applied to each panel. At that load, back-to-back axial strains near the four corners of each specimen were monitored. The lower platen, which is seated on a spherical ball, was adjusted so that the difference between the monitored strains were within one percent of the expected failure strain. Even though care was taken to mount the steel angles on the specimen so that the specimen ends would be flat and parallel, in several cases, adjustment of the platen was not sufficient, and metal shims were placed between

the steel angles and heated platen to achieve the desired strain uniformity.

An insulated clamshell-type oven with fin-strip heaters and fans mounted on the inside surfaces was used along with the heated platens to provide a uniform test temperature for the elevated temperature tests. Three thermocouples mounted on the inside surface of the oven and on the upper and lower platens were used as input for the three zone thermal controller. Thermocouples mounted on the test specimen were also monitored to ensure a uniform test article temperature prior to application of mechanical loads. Heat input was adjusted such that all thermocouple readings were within 25 degrees of the desired test temperature. For the elevated temperature tests, the specimens were heated while the test machine was in load control and maintaining an approximate load of 300 lb. Once the desired test temperature was achieved, the test specimen was loaded at a constant displacement rate of 0.02 in/min. Applied load, ram displacement, and back-to-back strains at the center of the panel were monitored in real-time. The tests were continued until the panels fractured.

Analysis

The ability to predict the panel test results was also investigated as part of this study. Several analysis approaches, with varying degrees of fidelity and hence complexity, were evaluated to determine their ability to reproduce the test results. Due to the lack of available data for IM7/5260, the design allowable strain determined at Boeing from coupon testing of IM7/5250, a material with properties considered identical to IM7/5260 for the design effort, was used in predicting failure modes and determining allowable design loads for each test temperature. A table containing the allowable strain data is presented in Table 2. The open-hole-compression average strain values of IM7/5250 were used as the design allowable strains of the IM7/5260 facesheets for the panels of this study.

The most basic analysis method used here was a one-dimensional strength of materials solution for the compressive strength. The method assumes that the applied load is a pure axial load uniformly distributed across the width of the panel and is the same for both facesheets (i.e., the panel is indeed flat). A further assumption is that the honeycomb core provides negligible stiffness in the axial direction. The strength of materials approach to the compressive strength reduces to the simple equation, $P = EA\varepsilon$, where P is the design load, $E = 8.63 \times 10^6$ psi is the isotropic modulus of elasticity of the facesheets determined from laminated plate theory, ε is the design allowable strain, and A is the effective cross-sectional area of the panel facesheets.

As a second step in increasing fidelity, two-dimensional finite element models were created. The test specimen was modeled as a composite multi-layer plate. A schematic drawing of the composite layers and their properties, used in the finite element model, are shown in Figure 5. The facesheets were modeled as separate quasi-isotropic lamina, the honeycomb was modeled as a single orthotropic layer, and the steel angle plates at each end were modeled as if they were continuously bonded to the facesheets. Although the steel angles were actually bolted to the composite panel, the approximations allowed for a very simplified plate model of the test specimen. The resulting finite element model consisted of 1113 nodes as displayed in Figure 6. The panel was first modeled and evaluated as a flat panel. A linear static analysis and linear buckling analyses were conducted using the general purpose finite element code NASTRAN (ref. 2). Two buckling analyses were performed to determine the range of possible buckling failure loads, one with assumed simply-supported end boundary conditions and a second analysis with assumed clamped end boundary conditions.

The effect of geometric imperfections was also investigated. Two of the panels were scanned prior to testing to determine the magnitude of their imperfections in the out-of-

plane direction. The out-of-plane imperfections for Panel 1 were measured along the length of the panel at the two unsupported edges. The out-of-plane imperfection was similar to, and consequently modeled as, a half cosine shape along the panel length. The amplitude of the imperfection was set equal to the average of the maximum out-of-plane measurements along the two edges, 0.045 inches. For Panel 2, the out-of-plane measurements were mapped to the grid of the nodal locations shown in Figure 6 to generate the initial imperfection for the finite element model. Figure 7 is a contour plot of the surface out-of-plane measurements for Panel 2. Note that this contour plot includes the pad up which accounts for a 0.036 inch contribution to the out-of-plane measurement after the ramp up to the joint area (see Figure 2). This pad up contribution was subtracted from the measurements before they were mapped to the nodal grid. For the geometric imperfection models, NASTRAN nonlinear analyses were utilized to evaluate the structural responses.

Results and Discussion

Since it is not practical to present all of the test data, only selected results are presented to describe the typical response of the panels under compression loading at room and elevated temperatures. Failure data along with pertinent panel characteristics are presented in Table 3. For all fourteen panels tested, failure of the panels occurred at the maximum applied load. Although the maximum strain was recorded at the failure load for all panels, the location of the maximum strain reading varied from panel to panel. It is important to note that, since a limited number of strain gauges were used during the tests, the measured maximum strains are not necessarily the maximum strains incurred by the panels during testing.

All 8-ply specimens failed due to facesheet fractures which is referred to as the facesheet strength failure mode. All panels referred to in Table 3 as having failed in the facesheet strength mode, were very similar in appearance. Figure 8 is a photograph of Panel 4 after failure which is typical of the appearance of all panels that failed in the facesheet strength mode. Increasing the test temperature from room temperature to 300°F did not appear to effect the failure mode for the 8-ply specimens. In comparing the failure data of the 8-ply titanium core panels with the 8-ply graphite-polyimide core panels, the effect of the type of core on the structural performance in compression is inconclusive.

For the 24-ply specimens, buckling of the panels prior to failure was observed for both the room and 250°F temperature tests, as indicated in Table 3. However, ultimate failure of the 24-ply panels at the room and the 250°F test temperatures was initiated by fracture of the facesheets well above the design allowable strain. Figure 9 is a photograph of Panel 11 which buckled prior to failure and is typical of the appearance of all failed 24-ply panels that experienced buckling before failure. For the 24-ply specimens, increasing the temperature from 250°F to 300°F resulted in a different failure mode. At 300°F, one 24-ply panel experienced a facesheet strength failure, and the other 24-ply panel experienced disbonding between the facesheet and core material. Figure 10 is a photograph of Panel 14 which failed in the disbond mode. The failure modes at 300°F can be attributed to a reduced strength of the facesheets and adhesive due to increasing temperature. Also, it is important to note that Panel 14 had potted ends only and thus did not have an associated clamp-up pressure that might prevent a disbond failure mode from occurring.

The maximum measured failure strain data for all the panels tested is displayed graphically in Figure 11, along with the laminate strain allowable data of Table 2. Ideally, all panels would be expected to fail at strains near the laminate unnotched allowable strain values for a given test temperature. From Figure 11, one can observe that the 24-ply panels achieved much greater measured strain levels then the 8-ply panels for the room and 250°F temperature tests. The maximum measured strains for the

24-ply were very close to the unnotched allowables. However, the 8-ply specimen maximum measured strains fell well below the unnotched allowable and displayed more scatter than the 24-ply panels. One 8-ply panel, Panel 5, failed with a maximum measured strain below the design allowable. When going from the 250°F test temperature results to the 300°F test temperature results, a dramatic, much greater than expected, decrease in the maximum strains were observed for the 24-ply specimens. At 300°F, the maximum strain for the 24-ply specimens fell well below the unnotched allowable level.

Figure 12 displays the failure load data for each panel tested as a function of temperature. Also plotted for comparison are the design loads calculated from a strength of materials approach. The design loads were calculated using the minimum specimen width which was 11.375 inches and 11.25 inches for the 8-ply and 24-ply specimens, respectively. A modulus of elasticity determined from lamination theory and based on ply properties and facesheet thicknesses based on a 0.0056 inch ply thickness for the IM7/5260 material were used in the computations. Although the failure loads for the 24-ply panels were above their design loads, there was not as large a difference between the design loads and measured loads as with the maximum design and measured strains. This is most likely attributable to panel bending which was ignored in the strength of materials approach described previously. The issue of bending is addressed later when the experimental data is compared to analysis results. As with the measured maximum strains, the failure loads for the 24-ply specimen showed a significant drop with increasing temperature, indicating a greater than expected strength reduction with increasing temperature to 300°F. For the 8-ply specimens, the test failure data showed greater scatter than obtained for the 24-ply specimens. The failure loads bracketed the design loads and several specimens failed at loads below the design load. Unlike the 24-ply specimens, no significant decrease in the failure load was observed at 300°F for the 8-ply specimens.

Back-to-back longitudinal strains measured at the center of the panel facesheets are shown with applied load for Panels 1, 5 and 11 in Figures 13-15, respectively. The experimental data shown in Figure 13 for Panel 1 is typical of most of the panels that failed in the facesheet strength mode or disbond mode. From Figure 13 it is apparent that a significant amount of bending was experienced prior to failure. As shown by the figure, back-to-back longitudinal strains diverge with increasing load. This panel bending can be attributed to geometric imperfections as discussed earlier. For Panel 5, Figure 14, bending was negligible, but the panel failed at a much lower load than the other two 8-ply panels tested at room temperature. The data shown in Figure 15 for Panel 11 is typical of the response obtained for all the panels that failed in the buckling mode. The diverging of the back-to-back strain measurements to the point where there is little increase in the load being carried by the panel as the facesheet strains continued to drastically increase and decrease on opposing facesheets is characteristic of panel buckling.

Analysis results are compared to experimental data in Figures 16–17, for Panels 1 and 2, respectively, which were the only two panels that were evaluated for geometric imperfections prior to testing. Shown in Figure 16 are the structural responses obtained for Panel 1. The strength of material approach assumes that the panel is perfectly flat to obtain a simplified linear solution. The linear buckling loads were obtained from the finite element model of the flat panel. The NASTRAN nonlinear structural analysis results include the effect of the geometric imperfections. The simply-supported boundary condition solution and the clamped boundary condition solution represent the two extreme conditions for edge support. Due to geometric imperfections which induce bending, the experimental data, and nonlinear analysis solutions diverge from the linear strength of

materials solution as the load is increased. In comparing the analysis solutions to the experimental data, the nonlinear analysis solution using the clamped boundary condition provides the better estimate of the load being carried by the panel at the design allowable strain value. The strength of materials approach over predicts the magnitude of the strain for a given applied load since it neglects the effect of the geometric imperfection and consequently bending of the panel. Although Panel 1, Figure 16, failed at a strain level greater that the design allowable, the load carried by the panel at failure was less than that predicted using the strength of materials approach primarily because of panel bending. The NASTRAN nonlinear analysis solution assuming the clamped end boundary condition provided the most accurate prediction of the experimental results. For Panel 2, Figure 17, the slope of the experimental curve at low loads is slightly greater than the slope obtained from the strength of materials prediction, indicating a higher than expected modulus of elasticity for the 8-ply laminate facesheets. Also, the panel failed at a load slightly below the design load for the panel.

In evaluating the test data, three critical issues arise. First, the maximum measured strain for the 8-ply specimens fell well below that of the 24-ply specimens for the room and 250°F temperature

tests. The 24-ply panels failed close to the unnotched allowable strain levels, however, there appeared to be a strength reduction related to the thinner, minimum gauge, 8-ply specimens. Consequently, specimens taken from 8-ply and 24-ply panel facesheets were prepared for coupon compression testing to determine any associated strength reduction due to the co-curing process for the thinner laminates. A total of sixteen 8-ply and sixteen 24-ply coupon specimens were cut from both facesheets of four of the panels tested. The coupon specimens were all cut 0.5 inches wide and 2.625 inches in length and were instrumented with back-to-back strain gauges. The core was carefully cut and ground away from the facesheets. Examination of the specimens revealed that the honeycomb core was indeed imbedded in the laminated facesheet material. Although much care was taken to apply a uniform axial compressive load to the specimens, bending was appreciable in most tests. The bending is believed to be due to a combined effect of geometric imperfections in the specimens and the asymmetry of the laminates due to the honeycomb core cutting into the inner surface and damaging the innermost layers of the laminate. Only two 24-ply specimens did not exhibit any significant bending prior to failure and hence were able to provide axial compressive strength data. For both specimens, an ultimate axial compressive strain of 10500 μin/in was measured. The ultimate compressive strain was above the design allowable but 12% below the unnotched allowable of 12000 μin/in. Bending was even more significant for the 8-ply specimens and unfortunately no comparable strength data was obtainable. The larger amount of bending observed for the 8-ply specimens could be attributed not only to a larger geometric imperfection effect, but to a more severe structural degradation effect of the honeycomb core cutting into the thin laminate.

The second critical issue concerns the dramatic decrease in the maximum measured strains and failure load for the 24-ply specimens in going from the 250°F tests to the 300°F tests. The possibility of an unexpectedly large strength reduction in the adhesive or core needs investigation. Finally, the failure of Panel 5, at such a low maximum measured strain and failure load, even below the design allowable, raises the issue of a possible manufacturing defect or a possible dramatic compressive strength reduction due to co-curing.

Concluding Remarks

Fourteen composite honeycomb sandwich panels were tested to failure under compressive loading at various test temperatures. The test

specimens included panels with both 8-ply and 24-ply graphite-bismaleimide facesheets and both titanium and graphite-polyimide core materials. For the majority of the panels, the load was introduced through fasteners loaded by steel angles representing double shear splice joints at both loaded ends of the panels. The structural compressive performance of the different panels were evaluated for room temperature, 250°F, and 300°F operating temperatures.

The 24-ply panels performed well in the room temperature and 250°F operating environments. Experimental results were fairly repeatable for the two panels tested at each test temperature. The panels experienced failure near the unnotched failure strains and far above the design allowable. The 24-ply panels experienced significant degradation of the panel strength in going from 250°F to the 300°F operating environment. Therefore, it is recommended that further study be conducted before utilizing the present 24-ply panel design at temperatures above 250°F.

The thinner 8-ply specimens did not perform as well as the 24-ply specimens. They experienced unexpectedly low failure strains and failure loads, in addition to much scatter in the failure data. Therefore, the present 8-ply panel design is not recommended as a reliable panel design in strength critical areas. However, one factor contributing to the scatter in the failure loads between each panel is the variation in the out-of-plane geometric imperfections and hence the degree of bending that each panel exhibits. Theoretically, the more bending a panel incurs, the lower the load for a given strain at the panel center. Coupon compression testing of specimens extracted from the panel facesheets was performed with limited success because these coupons also exhibited large amounts of bending. Bending of the coupon specimens was believed to be due to geometric imperfections and to the laminates being unsymmetric as a result of the honeycomb core cutting into the facesheet laminates during co-curing. The latter effect is believed to have caused a strength reduction in the facesheets.

References

1. Williams, Louis J.: HSCT Research Gathers Speed. Aerospace America, April 1995, pp. 32–37.

2. MSC/NASTRAN User Guide, Version 68, The Macneal-Schwendler Corporation, March 1994.

Table 1. Description or Test Specimens

Panel	Facesheet			Honeycomb core			Panel dimensions		Test temp, °F
	Material	Layup	No. plies	Material	Depth, in.	Density lb/ft^3	Length, in.	Width, in.	
1	IM7/5260	$(45/-45/0/90)_s$	8	Ti	1	6	35	11.875	RT
2	IM7/5260	$(45/-45/0/90)_s$	8	Ti	1	6	35	11.750	250
3	IM7/5260	$(45/-45/0/90)_s$	8	Ti	1	6	35	11.375	300
4	IM7/5260	$(45/-45/0/90)_s$	8	Ti	1	6	35	11.563	250
5	IM7/5260	$(45/-45/0/90)_s$	8	HFT-G	1	6	35	12.000	RT
6	IM7/5260	$(45/-45/0/90)_s$	8	HFT-G	1	6	35	12.000	250
7	IM7/5260	$(45/-45/0/90)_s$	8	HFT-G	1	6	35	12.000	300
8	IM7/5260	$(45/-45/0/90)_s$	8	HFT-G	1	6	35	12.000	RT
9	IM7/5260	$(45/90/-45/0)_{3s}$	24	HFT-G	1	6	36	12.063	RT
10	IM7/5260	$(45/90/-45/0)_{3s}$	24	HFT-G	1	6	36	12.000	300
11	IM7/5260	$(45/90/-45/0)_{3s}$	24	HFT-G	1	6	36	11.438	250
12	IM7/5260	$(45/90/-45/0)_{3s}$	24	HFT-G	1	6	36	12.000	250
[a]13	IM7/5260	$(45/90/-45/0)_{3s}$	24	HFT-G	1	6	36	12.000	RT
[a]14	IM7/5260	$(45/90/-45/0)_{3s}$	24	HFT-G	1	6	36	11.250	300

[a]Panel has potted ends with no joint attachment.

Table 2. Compressive Allowable Strain Data Used for IM7/5260 Laminates

Temperature, °F	Compressive allowable strains	
	Unnotched, μin/in	Design, μin/in
70	12 000	6500
250	10 440	5725
300	9 900	5400

Table 3. Experimental Failure Data

Panel	Plies	Core	Failure load, kips	Maximum strain, μin/in	Failure mode
Room temperature tests					
1	8	Titanium	–58.3	–8 845	Facesheet strength
5	8	Composite	–46.8	–5 907	Facesheet strength
8	8	Composite	–65.2	–9 641	Facesheet strength
9	24	Composite	–193.6	–12 324	Buckling
[a]13	24	Composite	–198.5	–11 555	Buckling
250°F test temperature					
2	8	Titanium	–48.5	–7 015	Facesheet strength
4	8	Titanium	–46.1	–7 132	Facesheet strength
6	8	Composite	–51.9	–7 022	Facesheet strength
11	24	Composite	–153.6	–10 346	Buckling
12	24	Composite	–164.3	–10 148	Buckling
300°F test temperature					
3	8	Titanium	–47.6	–7 146	Facesheet strength
7	8	Composite	–58.6	–8 687	Facesheet strength
10	24	Titanium	–142.6	–7 462	Facesheet strength
[a]14	24	Composite	–142.9	–8 146	Disbond

[a]Panel had potted ends with no joint attachment.

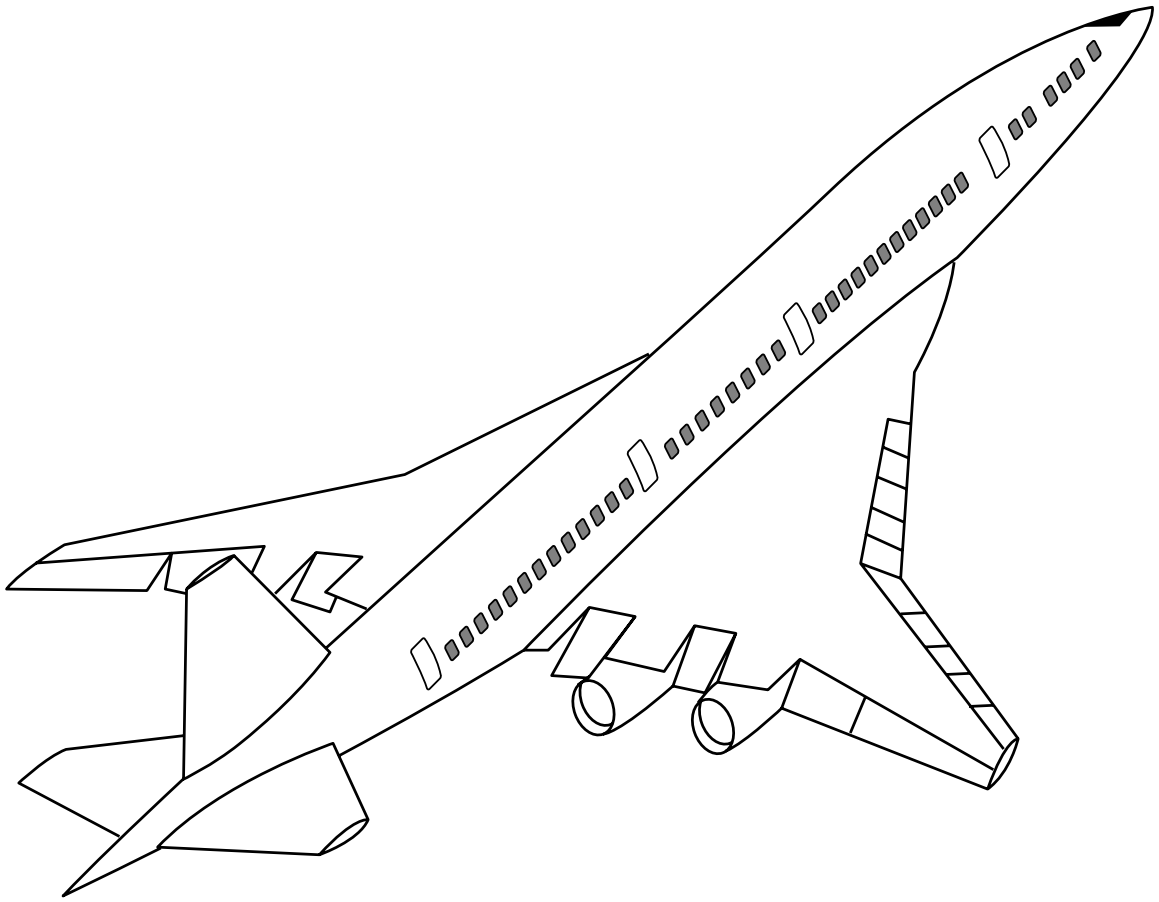

Figure 1. Illustration of a high speed civil transport concept.

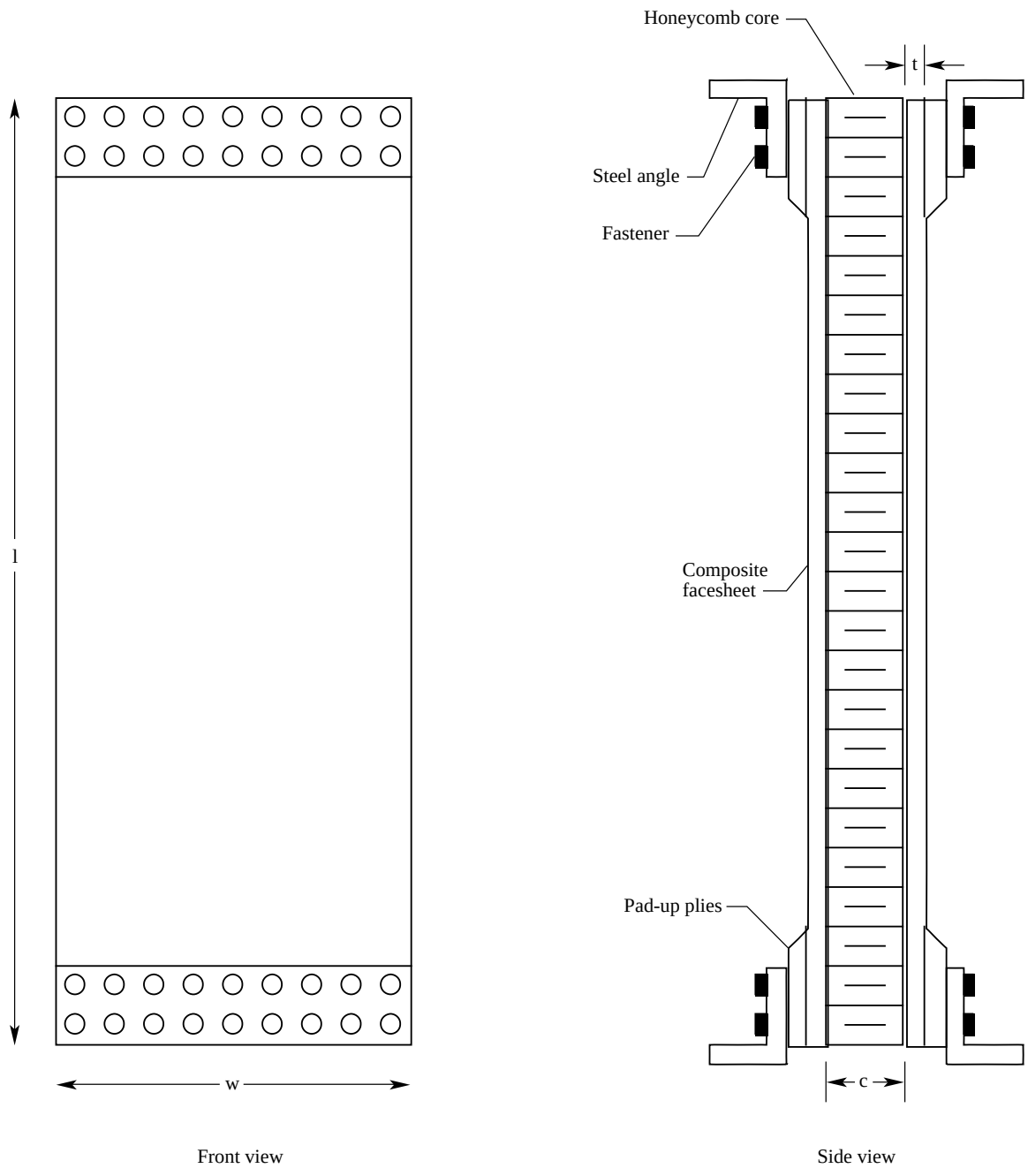

Figure 2. Schematic diagram of test specimen. Note: drawing is not to scale.

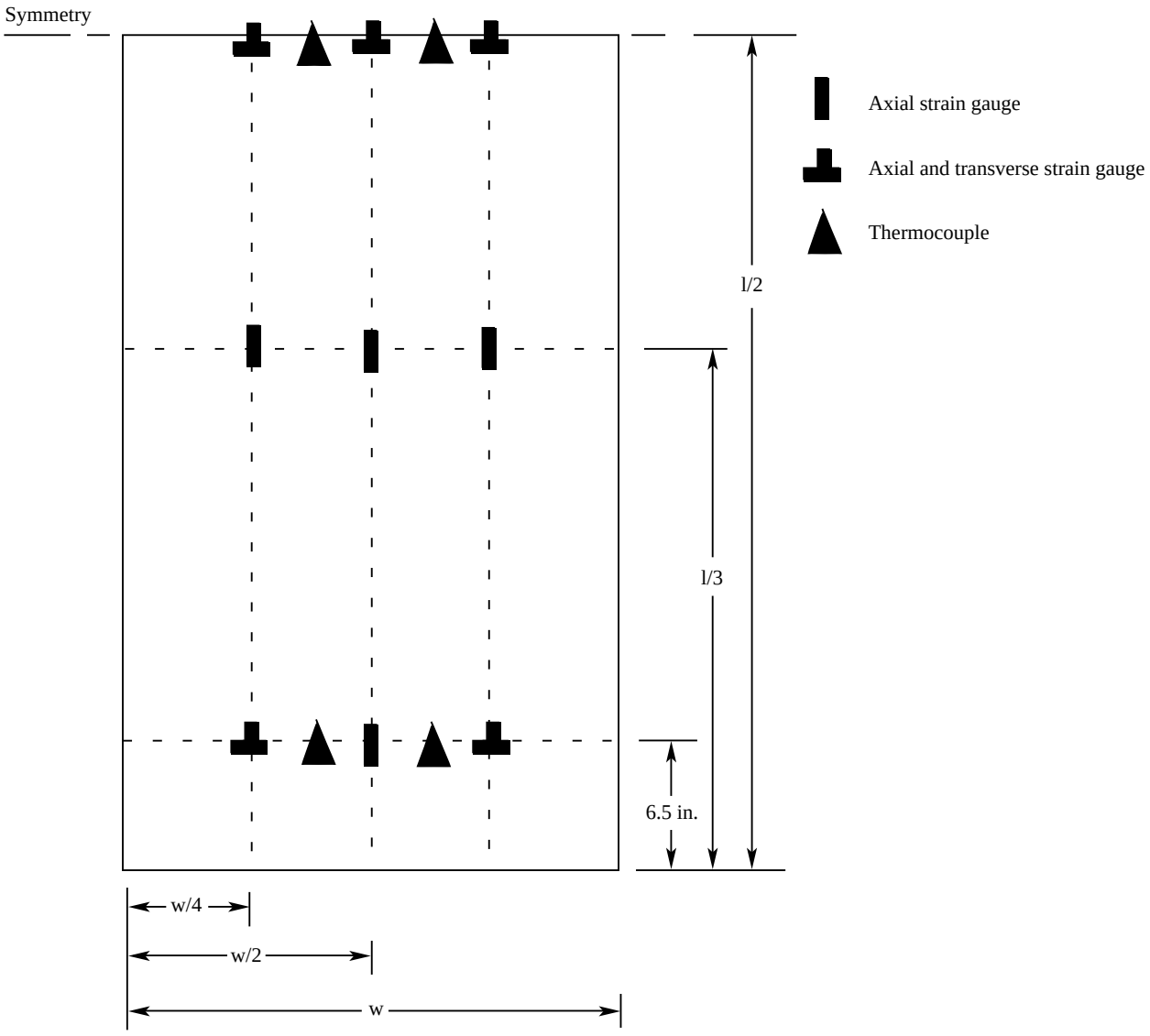

Figure 3. Typical instrumentation diagram where all gauges are mounted back-to-back and mirrored in the length, l, direction.

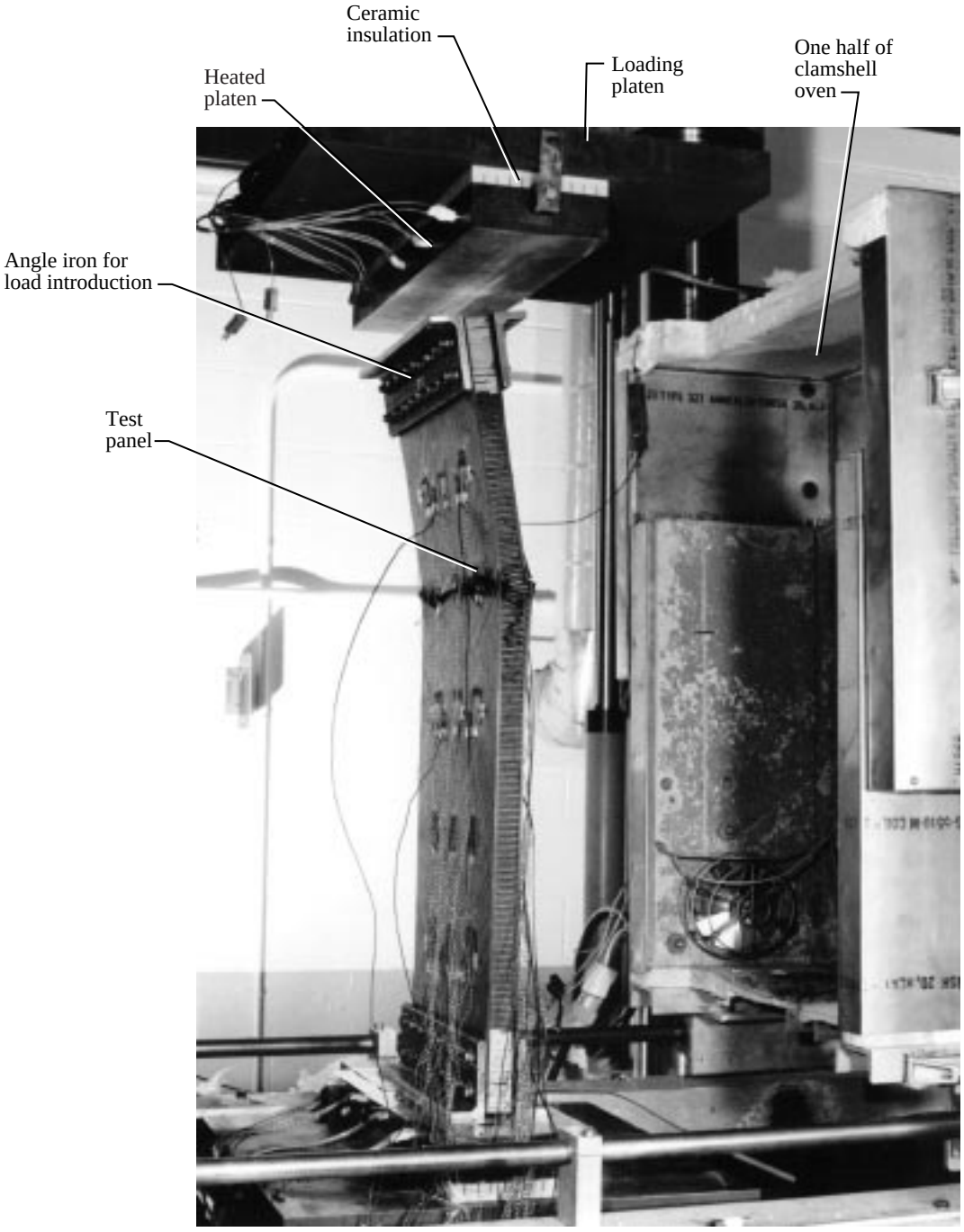

Figure 4. Photograph of failed panel located in test stand.

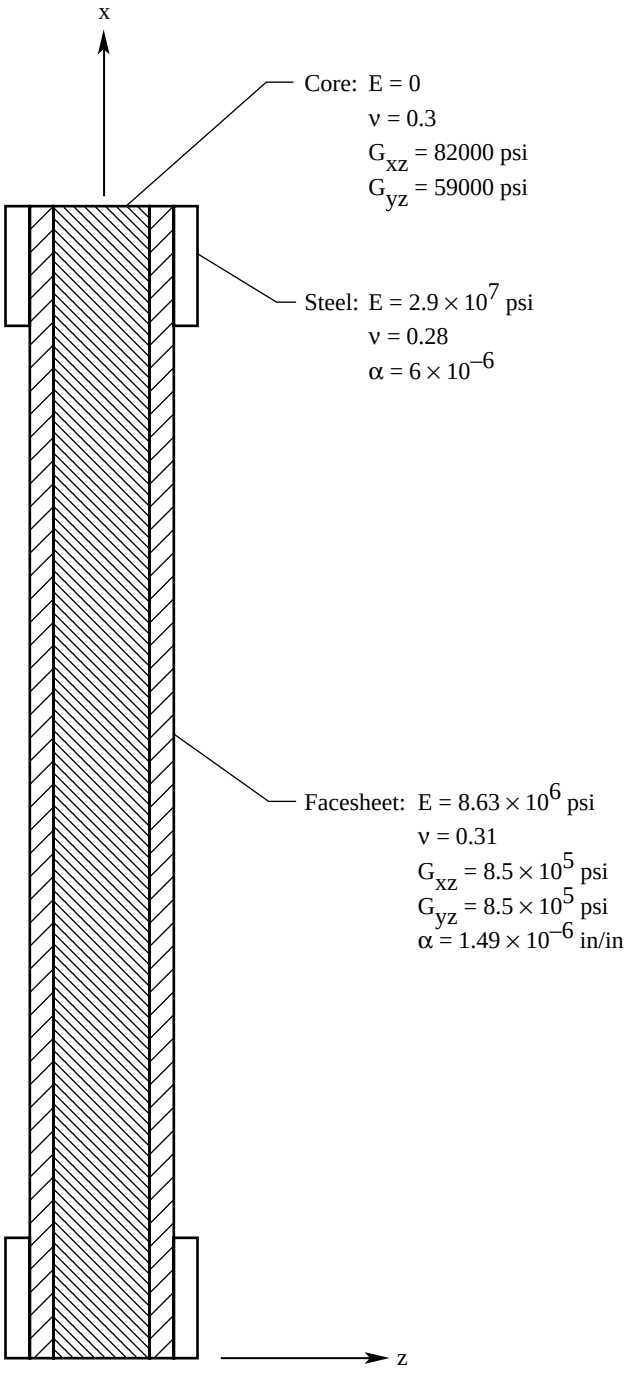

Figure 5. Schematic diagram of layers represented in the composite plate finite element model and their material properties. Note: drawing is not to scale.

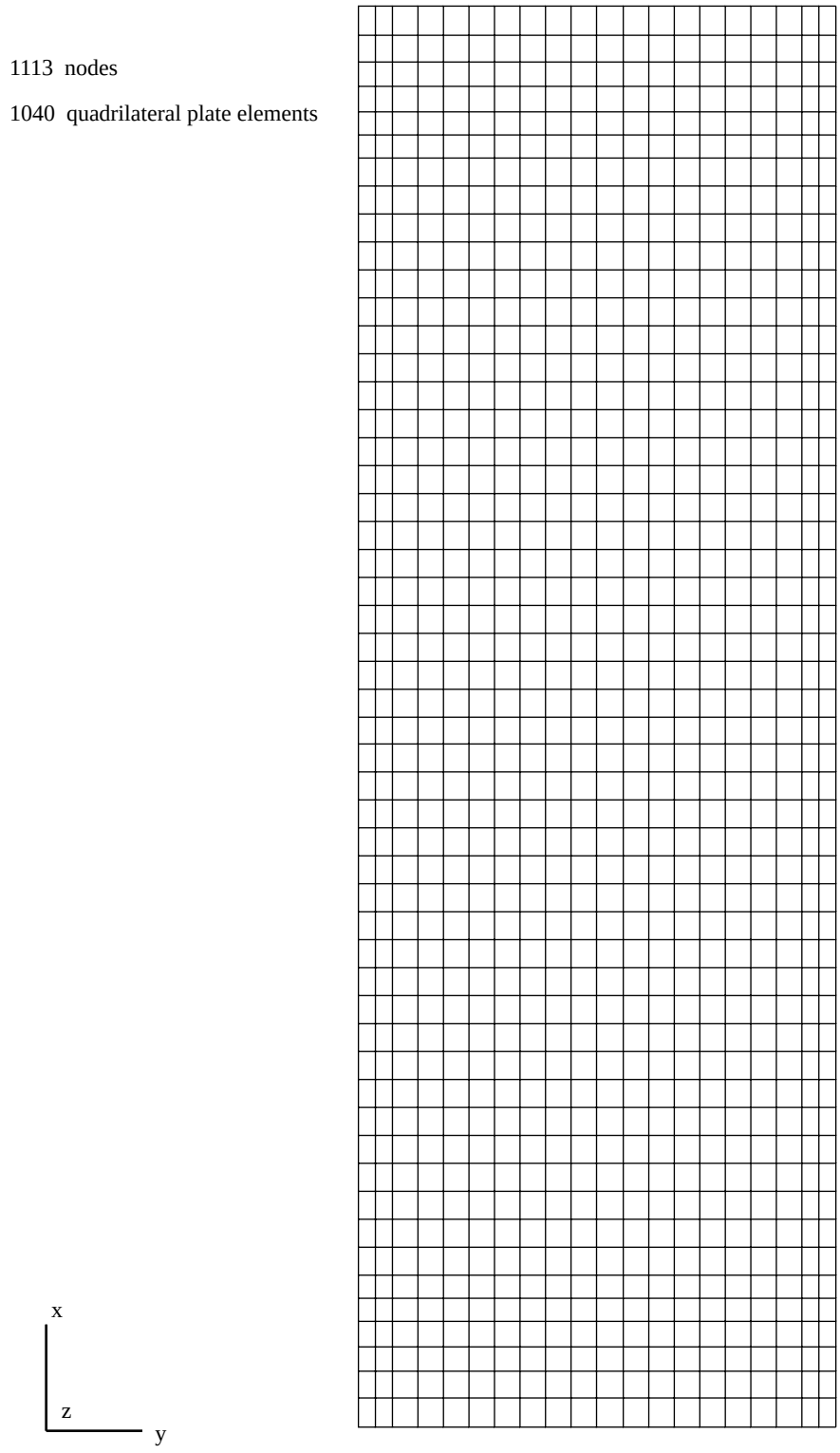

Figure 6. Finite element model of composite panel.

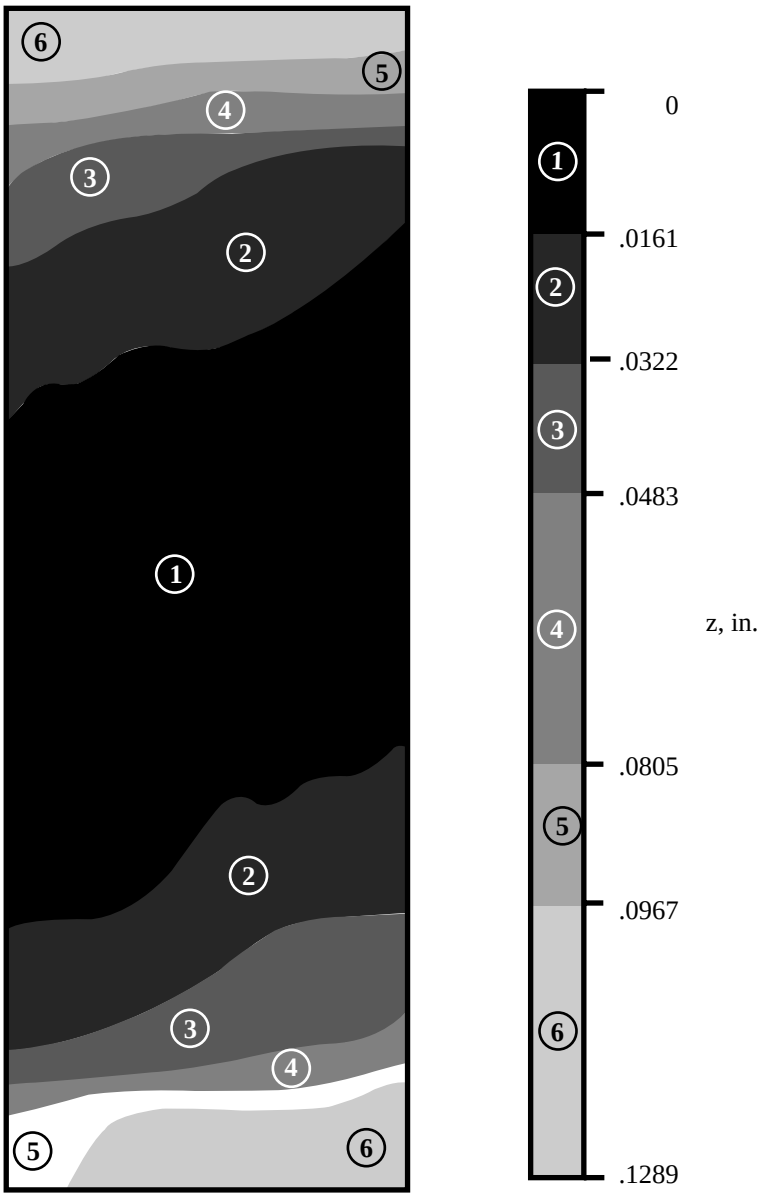

Figure 7. Contour plot of Panel 2 out-of-plane measurements.

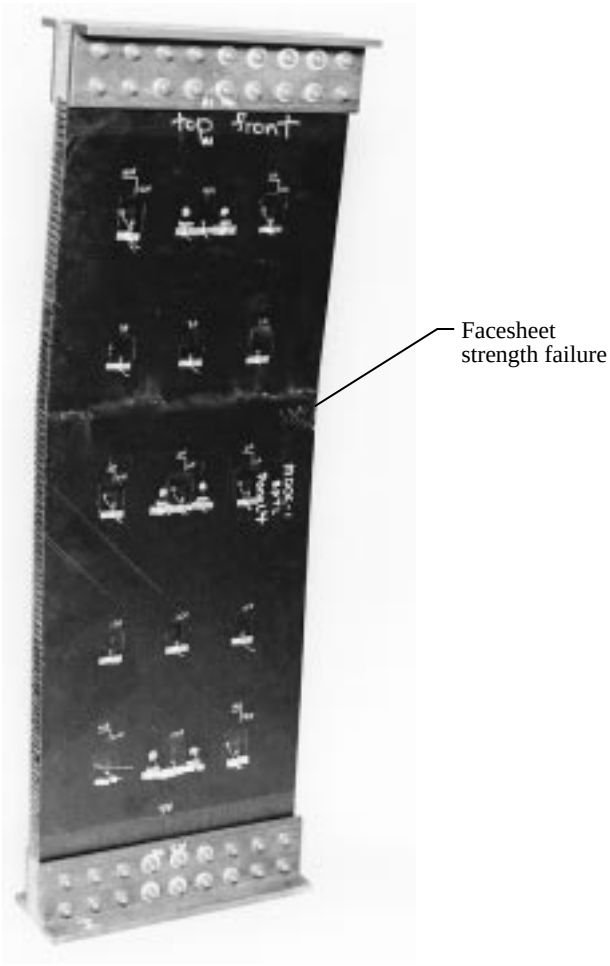

Figure 8. Photograph of Panel 4, with 8-ply facesheets, after testing to failure.

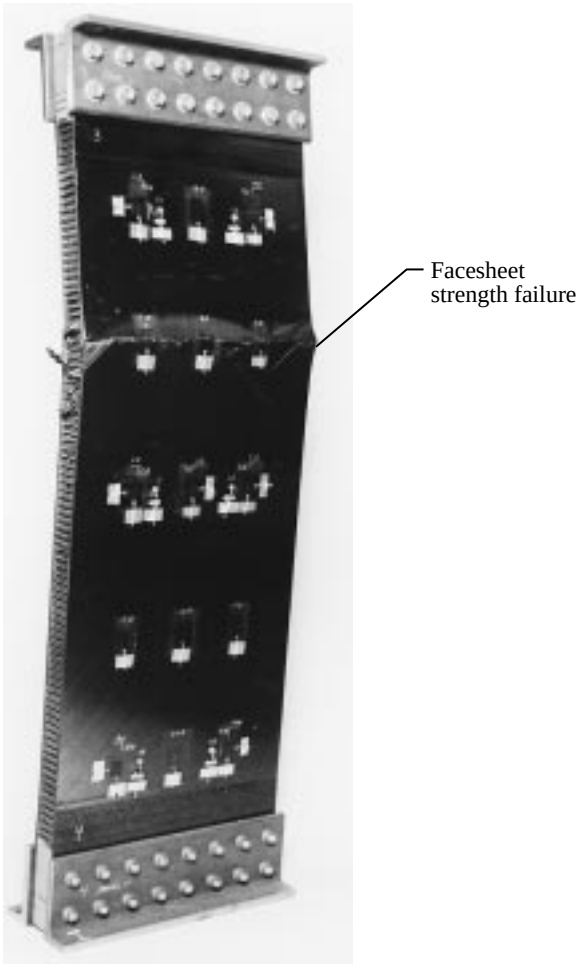

Figure 9. Photograph of Panel 11, with 24-ply facesheets, which buckled prior to failure.

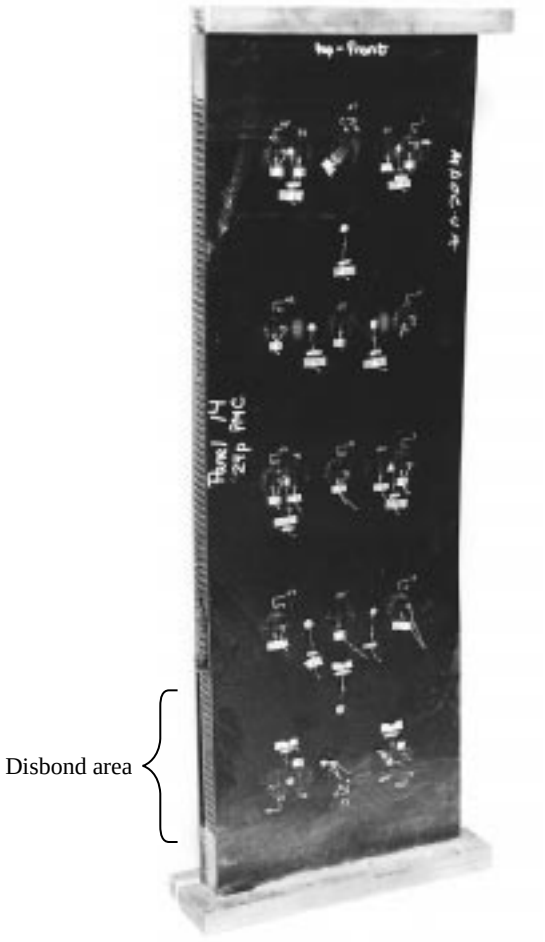

Figure 10. Photograph of Panel 14, with 24-ply facesheets and potted ends only, after testing to failure.

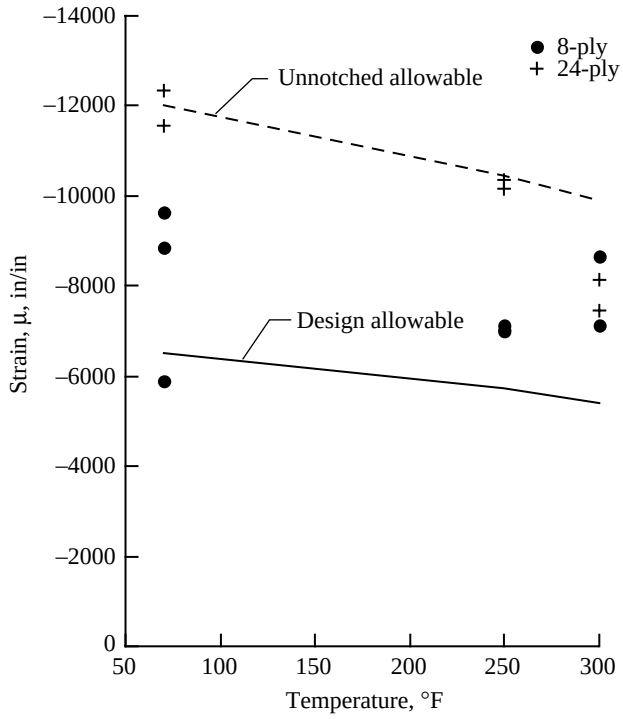

Figure 11. Maximum measured failure strain data.

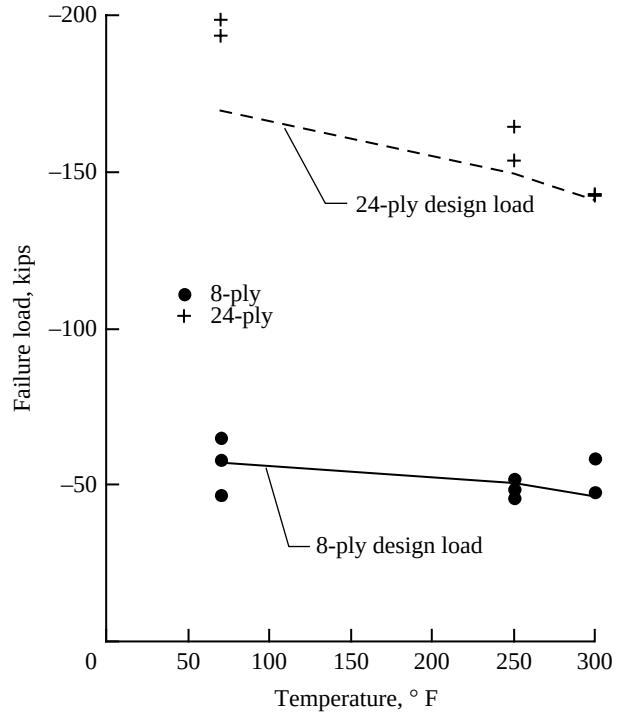

Figure 12. Panel failure load test data.

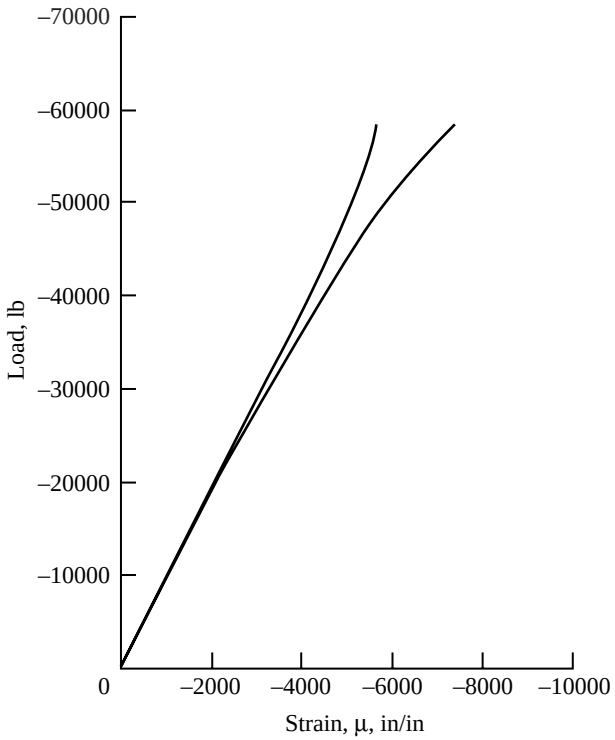

Figure 13. Back-to-back measured strains at center of panel facesheets for Panel 1 having 8-ply facesheets.

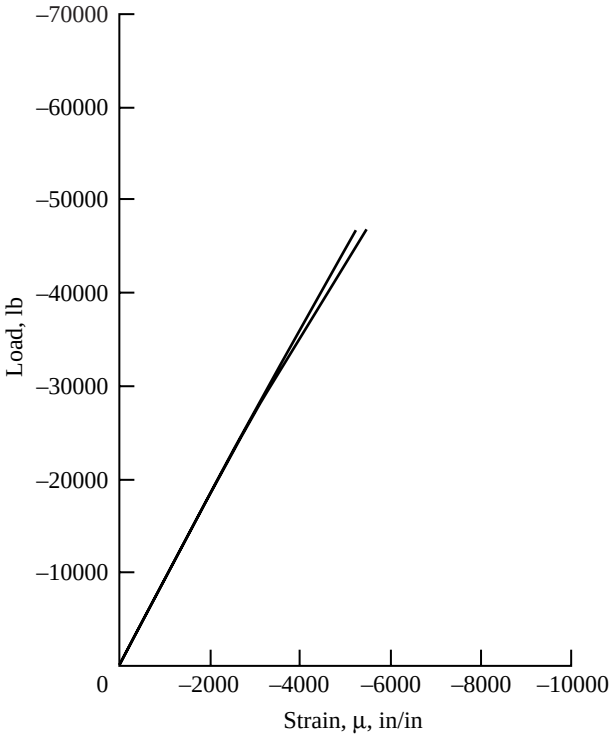

Figure 14. Back-to-back measured strains at center of panel facesheets for Panel 5 having 8-ply facesheets.

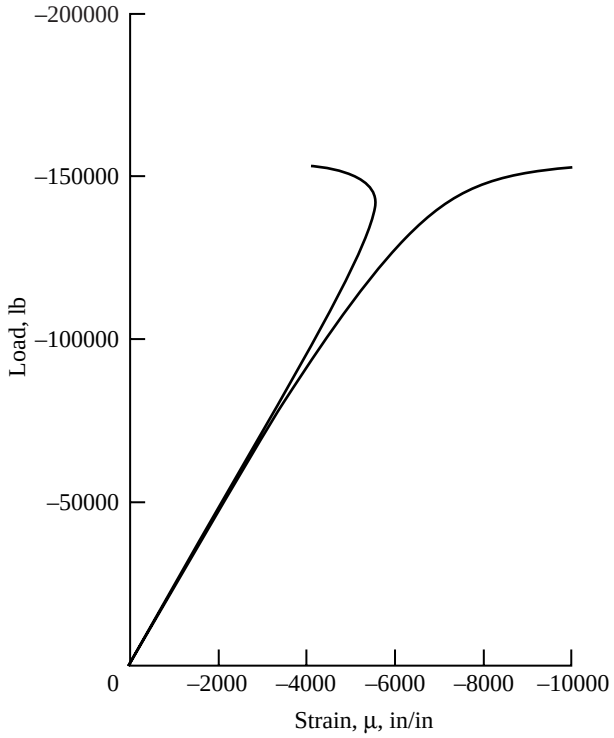

Figure 15. Back-to-back measured strains at center of panel facesheets for Panel 11 having 8-ply facesheets.

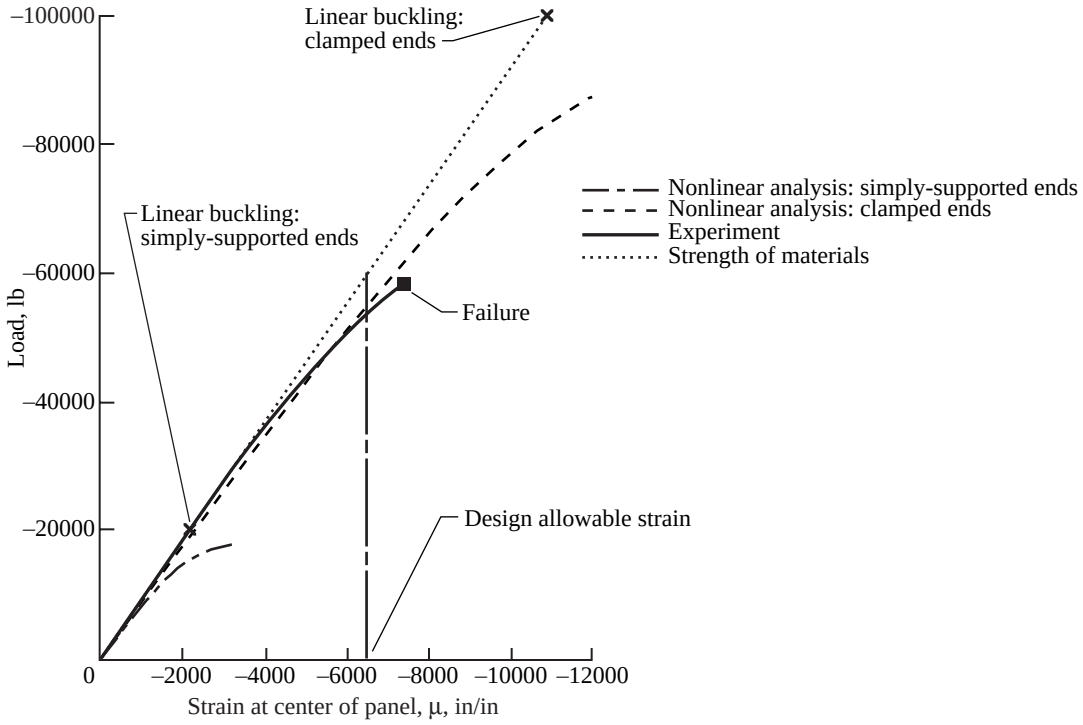

Figure 16. Room temperature NASTRAN nonlinear composite plate finite element analysis for Panel 1 (Geometric imperfection modeled from first cosine shape buckling mode).

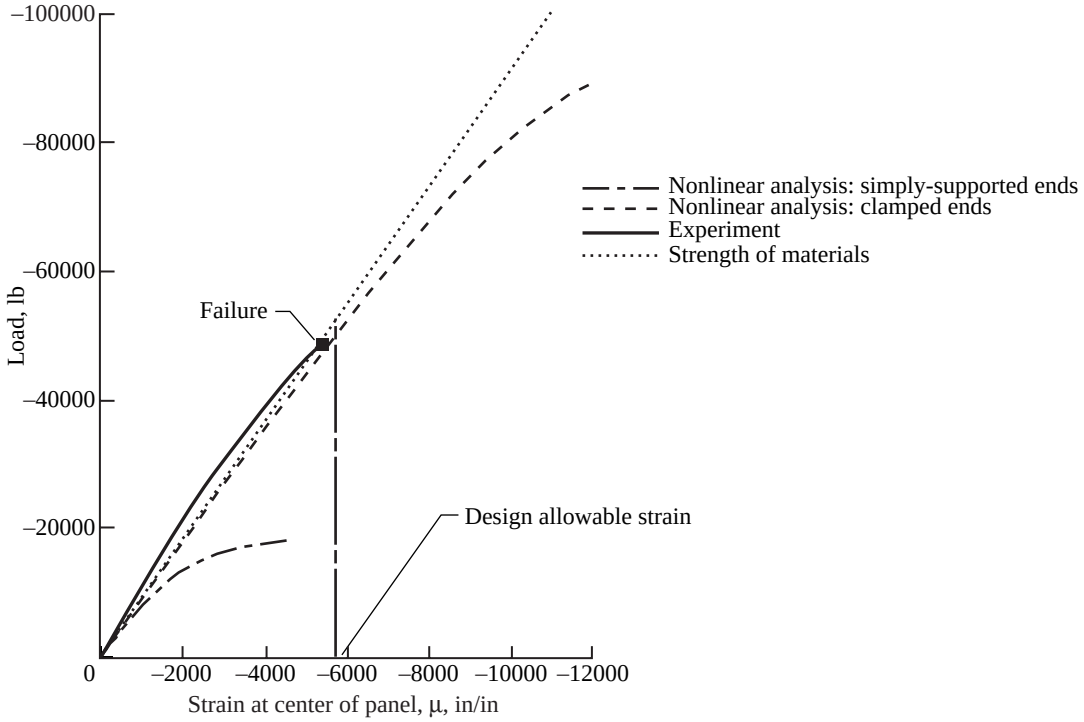

Figure 17. NASTRAN nonlinear composite plate finite element analysis for Panel 2 at 300°F (Geometric imperfection modeled from actual out of plane measurements mapped to nodal points).

REPORT DOCUMENTATION PAGE

Form Approved
OMB No. 0704-0188

1. AGENCY USE ONLY (Leave blank)	2. REPORT DATE	3. REPORT TYPE AND DATES COVERED
	April 1998	Technical Publication

4. TITLE AND SUBTITLE
Evaluation of Composite Honeycomb Sandwich Panels Under Compressive Loads at Elevated Temperatures

5. FUNDING NUMBERS
537-06-34-20

6. AUTHOR(S)
Sandra P. Walker

7. PERFORMING ORGANIZATION NAME(S) AND ADDRESS(ES)
NASA Langley Research Center
Hampton, VA 23681-2199

8. PERFORMING ORGANIZATION REPORT NUMBER
L-17666

9. SPONSORING/MONITORING AGENCY NAME(S) AND ADDRESS(ES)
National Aeronautics and Space Administration
Washington, DC 20546-0001

10. SPONSORING/MONITORING AGENCY REPORT NUMBER
NASA/TP-1998-207645

11. SUPPLEMENTARY NOTES

12a. DISTRIBUTION/AVAILABILITY STATEMENT
Unclassified-Unlimited
Subject Category 27 Distribution: Standard
Availability: NASA CASI (301) 621-0390

12b. DISTRIBUTION CODE

13. ABSTRACT (Maximum 200 words)
Fourteen composite honeycomb sandwich panels were tested to failure under compressive loading. The test specimens included panels with both 8 and 24-ply graphite-bismaleimide composite facesheets and both titanium and graphite-polyimide core materials. The panels were designed to have the load introduced through fasteners attached to pairs of steel angles on the ends of the panels to simulate double shear splice joints. The unloaded edges were unconstrained. Test temperatures included room temperature, 250F, and 300F. For the room and 250F temperature tests, the 24-ply specimen failure strains were close to the unnotched allowable strain values and failure loads were well above the design loads. However, failure strains much lower than the unnotched allowable strain values, and failure loads below the design loads were observed with several of the 8-ply specimens. For each individual test temperature, large variations in the failure strains and loads were observed for the 8-ply specimens. Dramatic decreases in the failure strains and loads were observed for the 24-ply specimens as the test temperature was increased from 250F to 300F. All 8-ply specimens appeared to have failed in a facesheet strength failure mode for all test temperatures. The 24-ply specimens displayed appreciably greater amounts of bending prior to failure than the 8-ply specimens, and panel buckling occurred prior to facesheet strength failure for the 24-ply room and 250F temperature tests.

14. SUBJECT TERMS
compression testing, composite honeycomb sandwich panels, elevated temperatures

15. NUMBER OF PAGES
29

16. PRICE CODE
A03

17. SECURITY CLASSIFICATION OF REPORT	18. SECURITY CLASSIFICATION OF THIS PAGE	19. SECURITY CLASSIFICATION OF ABSTRACT	20. LIMITATION OF ABSTRACT
Unclassified	Unclassified	Unclassified	